



An off-axis Golay3 sparse aperture telescope with a freeform secondary mirror

Junliu Fan¹ · Quanying Wu¹ · Baohua Chen¹ · Weimin Shen²

Received: 17 November 2018 / Accepted: 12 March 2019 / Published online: 17 April 2019
© The Optical Society of Japan 2019

Abstract

The application of freeform surface in an optical system can effectively increase the freedom of optical design and reduce the number of optical elements. In this work, a two-mirror off-axis sparse aperture telescope is proposed. The primary mirror is made of three sub-mirrors arranged in the Golay3 configuration while the secondary is a freeform surface defined by a polynomial of two variables X and Y . The off-axis configuration is used to remove the obstruction of the secondary mirror. The results indicate that the fill factor of the Golay3 primary mirror increases to 58.4%, which is significantly higher than that of the on-axis configuration. The image quality is improved within 2.5° full field of view from its spot diagram, distortion, modulation transfer function, and encircled energy.

Keywords Sparse aperture · Freeform · Field of view · Fill factor

1 Introduction

Sparse aperture (SA) optical imaging system is comprised of several small apertures to approximate a large equivalent monolithic aperture [1, 2]. In addition to maintaining the equivalent resolving power of a monolithic aperture imaging system, a SA system has the advantages of light weight, small size, and low manufacturing cost. The SA systems can be divided into two types. The first is the multiple-mirror telescope (MMT) in which several small mirrors resolve an object and share the same secondary mirror [3]. The other is the multi-telescope telescope (MTT) system that is made of several small and independent telescope systems [4].

For a MMT SA system, especially for an on-axis one (Cassegrain or Gregorian), misalignment among the sub-mirrors and residual aberrations of the optical design are the most fundamental error sources which severely limit the useful field of view (FOV) [5, 6]. For ground-based MMT

SA systems, the FOV is about 5 arcseconds at a wavelength of 500 nm (so-called isoplanatic patch) and increases with the wavelength at a power of 1.2 [7]. For space-based SA systems, the FOV could be much larger. However, the FOV needs to be even larger for many applications when extensive objects are observed.

For a SA system, the fill factor is defined as the ratio of all sub-mirrors' area to that of their surrounding aperture. The change of the fill factor will affect the system's modulation transfer function (MTF) enormously. Due to the central obstruction caused by the secondary mirror, the fill factor of an on-axis two-mirror SA system is relatively small. This decreases the mid-spatial frequency in the modulation transfer function (MTF) and could lead to missing a fainter object that locates near a brighter one [8–10]. To overcome the shortcomings of an on-axis SA system, the off-axis SA system is used in which the optical elements are either tilted or decentered to avoid the central obstruction [11]. As a result, the fill factor is significantly improved at a price of high-order coma, astigmatism and other field-dependent aberrations. For the convenience of manufacturing and fabrication, the surface of the sub-mirrors of an MMT SA system is usually chosen to be spherical which makes it more difficult to balance these aberrations. Although it is effective to balance the aberrations and enlarge the FOV [12], a refractive field corrector may cause the bothering chromatic aberrations, especially for a system with a high F /number.

✉ Quanying Wu
wqcyh@mail.usts.edu.cn

¹ Jiangsu Key Laboratory of Micro and Nano Heat Fluid Flow Technology and Energy Application, School of Mathematics and Physics, Suzhou University of Science and Technology, Suzhou 215009, Jiangsu, China

² School of Optoelectronic Science and Engineering, Soochow University, Suzhou 215009, Jiangsu, China

Compared with the traditional surface, the freeform surface is more advantageous in correcting the asymmetrical aberrations especially for an off-axis system with a wide FOV [13]. It provides more variable parameters for the optical design and hence has the potential to achieve a larger FOV with less optical elements. Typically, a freeform surface is represented by a suitable mathematical expression that can be decomposed into rotationally symmetric and asymmetric parts [14, 15].

In this paper, a new design of a two-mirror off-axis MMT is presented. The primary mirror (PM) of the off-axis MMT is composed of three identical sub-mirrors and the secondary mirror (SM) is adopted a freeform surface that is a combination of X – Y polynomials and the basic conic surface expression. The new MMT can achieve a full diagonal FOV of 2.5° and a fill factor of nearly 58.4%.

2 The X – Y polynomials of the freeform secondary mirror

Compared with surfaces of rotationally asymmetry, the freeform surfaces have more freedom of optical design and are capable of reducing the number of optical surfaces

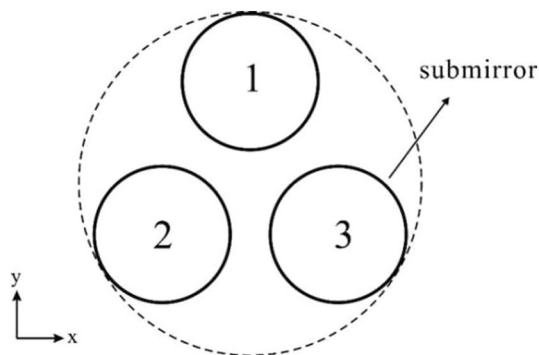


Fig. 1 The layout of the Golay3 SA

and the complexity of the optical system. There are several mathematical descriptors for the design of a freeform optical system, such as the anamorphic sphere, X – Y polynomials, Zernike polynomials, Gaussian basis function and so on [16]. The XY and Zernike polynomials are relatively more advantageous in correcting the asymmetric aberrations among all the mathematical descriptors. Combined with the ability of aberration correction and the association with the actual machining, we used the X – Y polynomial of rotationally asymmetric surface for the secondary mirror in this work. The polynomial has high degree of freedom and can be expanded into monomials of $x^m y^n$, here $m + n \leq 10$.

$$z = \frac{c(x^2 + y^2)}{1 + \sqrt{(1 - (1 + k)c^2(x^2 + y^2))}} + \sum_{j=2}^{66} c_j x^m y^n, \tag{1}$$

$$j = [(m + n)^2 + m + 3n] / 2 + 1. \tag{2}$$

Here z is the sag of the surface along the local z -axis, x and y the coordinates in the local coordinate system of the freeform surface, c the vertex curvature, and k the conic constant. Once given a reasonable starting point, the curvatures, conics, and the parameters c_j are set as variable parameters and optimized with the optical software ZEMAX which uses the damped least square (DLS) algorithm to improve the telescope design. For an off-axis optical system, the starting point is an on-axis one which is firstly optimized to obtain the correct first-order parameters. During the design process, we use a progressive design strategy to approach the design requirements. Besides, successful optimization of a freeform system also depends on suitable optimization constraints which are detailed in Sect. 3.

The layout of the Golay3 SA primary mirror is illustrated in Fig. 1. Due to the YZ -plane symmetry, the two-mirror off-axis SA system is optimized over half of the FOV. The FOV is sampled in a rectangular grid instead of linear sampling in the radial direction of a rotationally symmetric system.

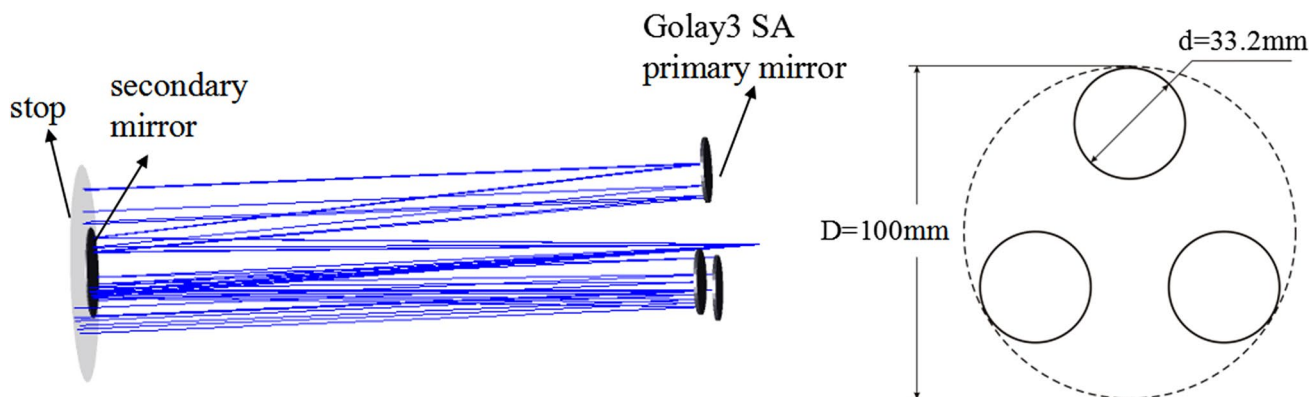


Fig. 2 The configuration of the on-axis Golay3 SA

3 The design process of the two-mirror off-axis Golay3 SA system

First, a two-mirror on-axis Golay3 SA system is determined based on the first-order optics and third-order aberration theory as illustrated in Fig. 2 [17]. The fill factor of this on-axis system is around 33%. As the FOV increases, the

size of the secondary mirror will increase to receive off-axis incident rays when the distance between the primary and the secondary mirrors remains unchanged. This will increase the obstruction of the central rays and reduce the fill factor of the system.

Therefore, we tilt the primary and secondary mirrors to reduce the central obstruction. The tilt parameters are

Fig. 3 The initial configuration of the off-axis Golay3 SA

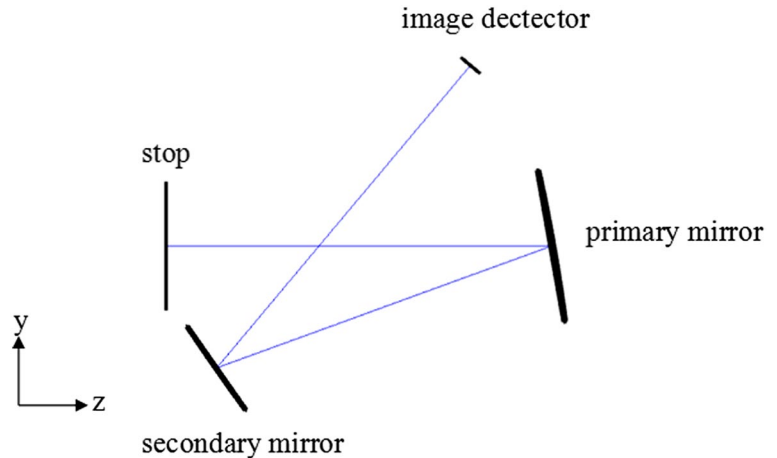


Table 1 Specifications of the proposed Golay3 SA

| Parameters | Value |
|-------------------------------------|--|
| Wavelength coverage | 0.5–2.0 μm |
| Diameter of primary mirror | 136 mm |
| Entrance pupil diameter | 100 mm |
| Full field of view(diagonal) | 2.5° |
| CCD pixel pitch | 20 μm |
| Image quality | MTF > 0.4 at the Nyquist frequency |
| Spot size (the shortest wavelength) | RMS radius < the size of one CCD pixel pitch |
| Distortion | < 0.5% at the maximum field |

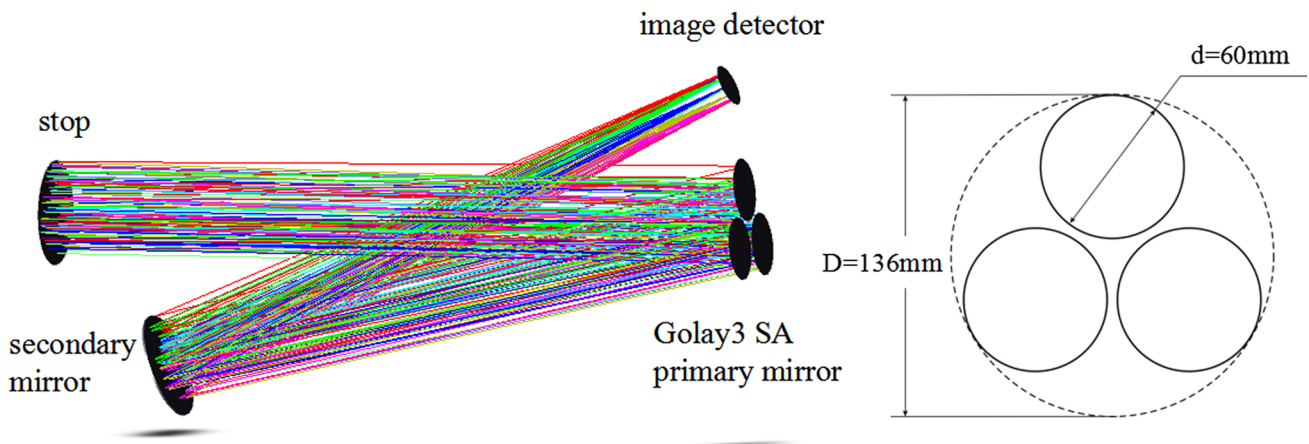


Fig. 4 The final configuration of the proposed off-axis Golay3 SA system

Table 2 Coefficients of the XY polynomial for secondary mirror

| Coefficient | Value | Coefficient | Value |
|-------------|--------------------------|--------------|--------------------------|
| Conic | 0.085 | $X^2 Y^5$ | -1.243×10^{-15} |
| $X^0 Y^1$ | -1.373×10^{-7} | $X^0 Y^7$ | 3.326×10^{-15} |
| $X^2 Y^0$ | -2.719×10^{-3} | $X^8 Y^0$ | -3.639×10^{-17} |
| $X^0 Y^2$ | -2.723×10^{-3} | $X^6 Y^2$ | -4.212×10^{-17} |
| $X^2 Y^1$ | 1.296×10^{-8} | $X^4 Y^4$ | -7.089×10^{-17} |
| $X^0 Y^3$ | 1.877×10^{-8} | $X^2 Y^6$ | -6.402×10^{-17} |
| $X^4 Y^0$ | -2.648×10^{-8} | $X^0 Y^8$ | -3.446×10^{-17} |
| $X^2 Y^2$ | -5.295×10^{-8} | $X^8 Y^1$ | -1.311×10^{-19} |
| $X^0 Y^4$ | -2.642×10^{-8} | $X^6 Y^3$ | -2.886×10^{-19} |
| $X^4 Y^1$ | -2.144×10^{-12} | $X^4 Y^5$ | 3.284×10^{-19} |
| $X^2 Y^3$ | 2.024×10^{-12} | $X^2 Y^7$ | 1.370×10^{-19} |
| $X^0 Y^5$ | -6.960×10^{-12} | $X^0 Y^9$ | -5.488×10^{-19} |
| $X^6 Y^0$ | -4.150×10^{-13} | $X^{10} Y^0$ | 2.927×10^{-21} |
| $X^4 Y^2$ | -1.428×10^{-12} | $X^8 Y^2$ | -2.723×10^{-21} |
| $X^2 Y^4$ | -1.378×10^{-12} | $X^6 Y^4$ | -2.834×10^{-21} |
| $X^0 Y^6$ | -4.488×10^{-13} | $X^4 Y^6$ | -6.286×10^{-21} |
| $X^6 Y^1$ | 1.169×10^{-15} | $X^2 Y^8$ | 2.215×10^{-21} |
| $X^4 Y^3$ | -2.602×10^{-17} | $X^0 Y^{10}$ | 3.931×10^{-21} |

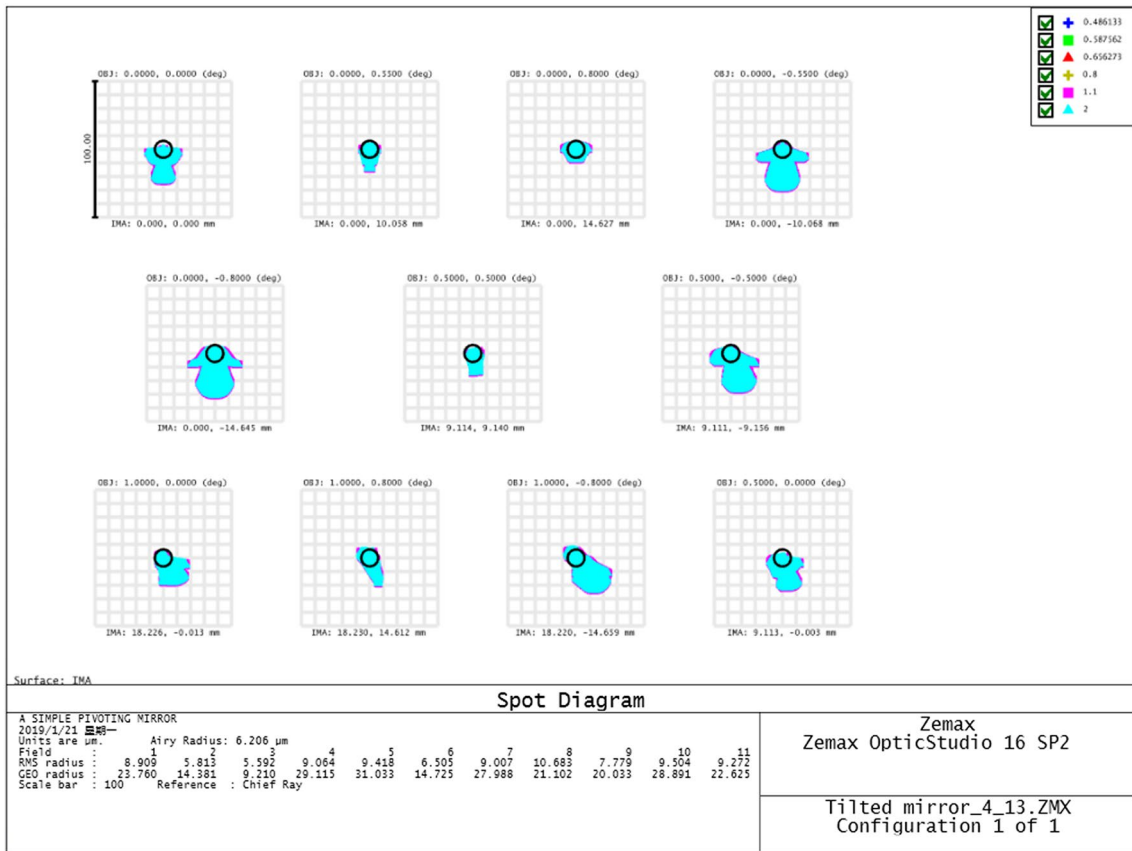


Fig. 5 Spot diagram of the off-axis Golay3 SA system

considered as variables and the constraints are set to ensure an unobstructed and compact system as shown in Fig. 3. During the optimization process, the top of the secondary mirror is first set to be at least 30 mm lower than the bottom of the Golay3 primary mirror and 70 mm right to the stop. Then the bottom of the image plane is set to be at least 100 mm above the top of the primary mirror. It is also important to optimize the system to meet the physical requirements such as the tube length and baffle. The entrance pupil is located at 760 mm in front of the Golay3 SA primary mirror to simplify the baffle design. During the optimization process, six representative wavelengths are chosen and they are 0.486, 0.587, 0.656, 0.800, 1.100 and 2.000 μm . Table 1 lists the specifications of the proposed off-axis Golay3 SA system.

4 Results and discussion

The layout of the proposed off-axis Golay3 SA MMT is shown in Fig. 4. The F/number of the optical system is 10.46 and its focal length is 1051.77 mm. The radii

of curvature of the primary and secondary mirrors are -3984.39 mm and 172.474 mm, respectively. The distance between primary mirror and secondary mirror is 685.92 mm while that between the secondary mirror and the image detector is 702.87 mm. The primary and secondary mirrors are tilted in the x direction by -4.99° and -5.60° , respectively, where the minus sign represents counterclockwise. The detailed surface data of the secondary mirror are presented in Table 2, and the normalization radius is 1 mm.

In the optical system the stop is located far away from the primary mirror. The secondary mirror and the image detector are tilted in such a way that a direct stray-light path from the object to the detector is prevented.

The optical performance of the off-axis SA system is assessed for the following representative FOVs ($0^\circ, 0^\circ$), ($0^\circ, \pm 0.55^\circ$), ($0^\circ, \pm 0.8^\circ$), ($0.5^\circ, 0^\circ$), ($0.5^\circ, \pm 0.5^\circ$), ($1^\circ, 0^\circ$), and ($1^\circ, \pm 0.8^\circ$). The spectrum of the SA system covers visible light and near infrared (NIR) region as well. The performance of the off-axis Golay3 SA system is evaluated using the criteria of the spot diagram, modulation transfer function (MTF), encircled energy and distortion.

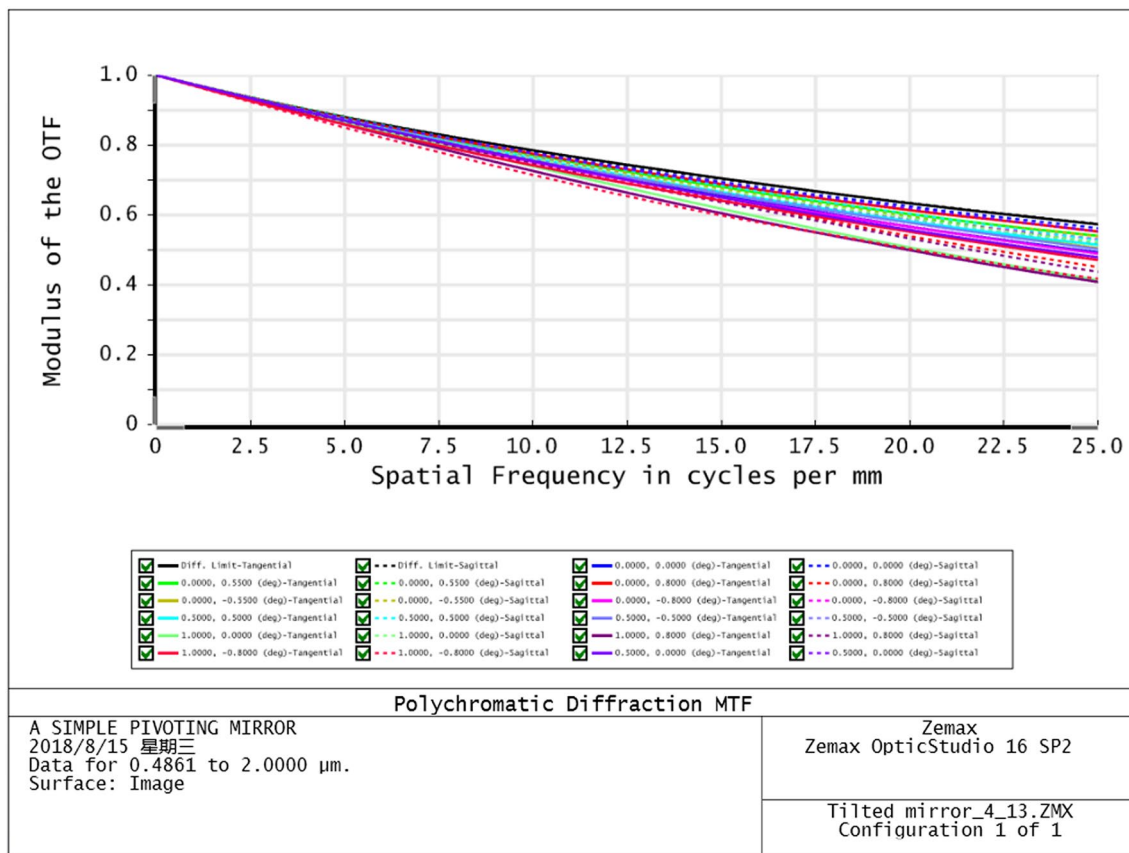


Fig. 6 MTF curves of the off-axis Golay3 SA system

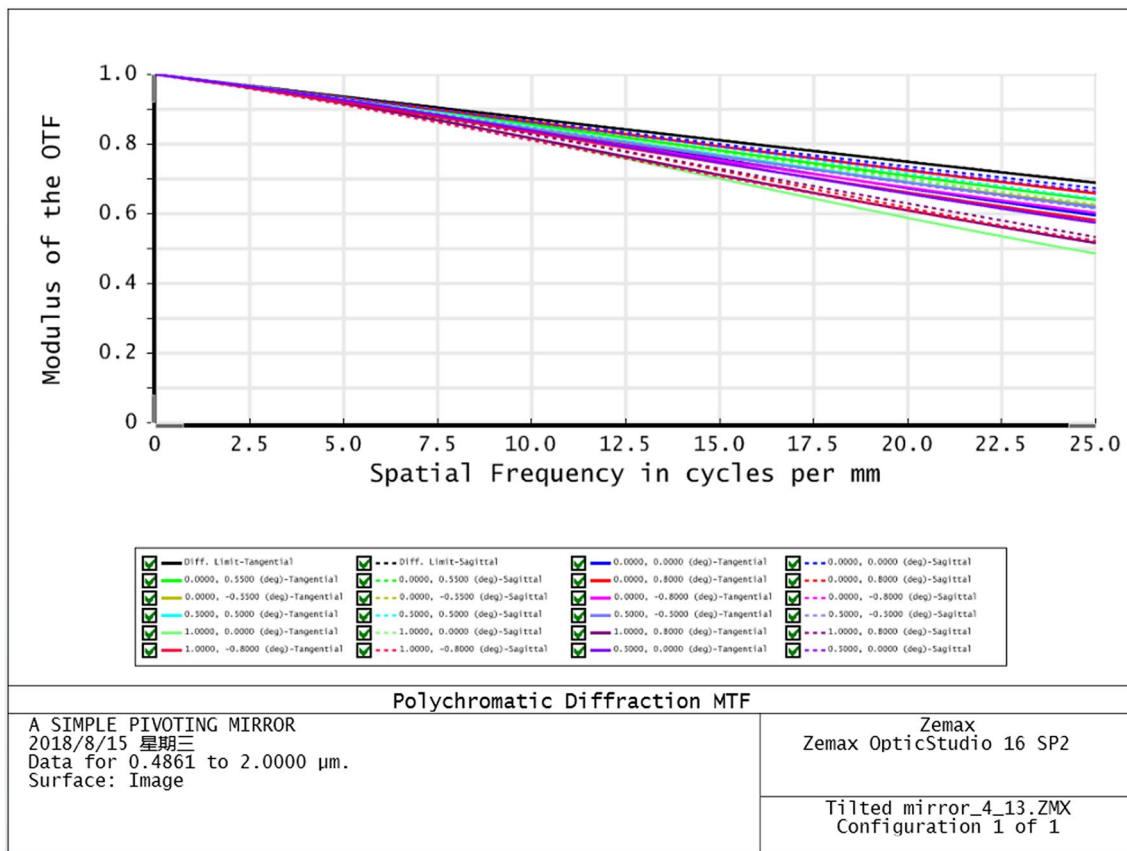


Fig. 7 MTF curves of the off-axis system with an equivalent monolithic aperture

The spot diagram is shown in Fig. 5. For the shortest wavelength (0.486 μm), the maximum root mean square (RMS) radius is 10.683 μm which is larger than 6.206 μm of the Airy disk radius, but still less than the size of one CCD pixel pitch. The system has no chromatic aberration seen from Fig. 5 because it is an all-reflective.

The MTF curves are presented in Fig. 6. The MTF values are greater than 0.4 at 25 line pairs/mm which correspond to the Nyquist frequency of the CCD pixel pitch. The diameter of each sub-mirror is 60 mm which contributes to a fill factor of 58.4%. The fill factor of the off-axis Golyay3 SA system is large enough that the first cutoff frequency usually characterized by a system with small fill factor does not appear. The MTF of the Golyay3 SA system does not lose too much information compared

with an equivalent monolithic aperture system as shown in Fig. 7.

Figure 8 shows an encircled energy plot for the off-axis Golyay3 SA system. For most FOVs, the encircled energy plots approach the diffraction limited, and 80% of the energy is contained within a diameter of 44 μm (nearly two times the size of the CCD pixel pitch), which is acceptable considering the fact that SA primary mirror collects less light energy than an equivalent monolithic mirror. The maximum distortion is -0.404% as shown in Fig. 9.

Figure 10 provides a departure in curvature of the secondary mirror after optimizing the coefficients of the X–Y polynomials. The curvatures of the freeform surface vary between $3.48\text{E}-4$ and $3.55\text{E}-4 \text{ mm}^{-1}$ within the range

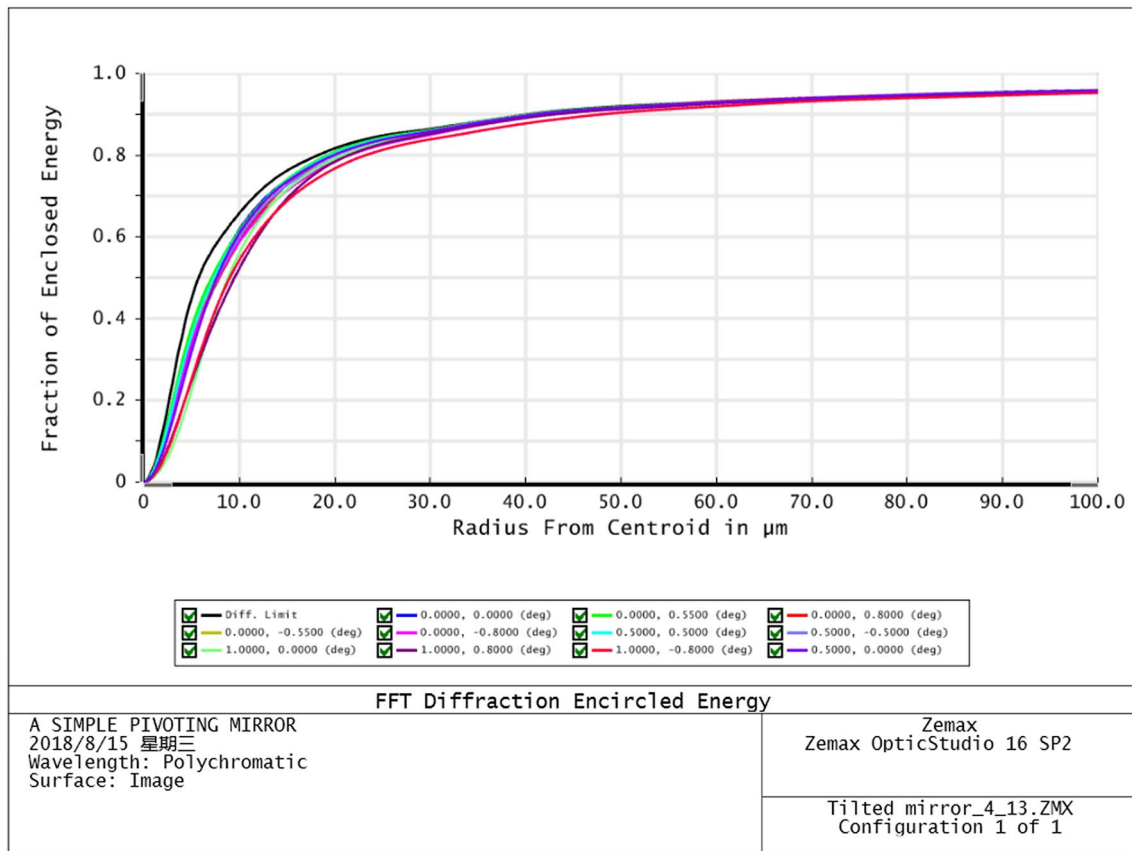


Fig. 8 The encircled energy plot of the off-axis Golyay3 SA system

(diameter of 100 mm), which ensures the feasibility of the manufacturability and testing of the secondary mirror.

For a two-mirror SA system, the adoption of an off-axis configuration with a freeform secondary mirror will achieve a large fill factor and a wide field of view compared with its on-axis counterpart. There is no doubt that the manufacturing, test and assembly cost of an off-axis optical system is much higher than the on-axis one. However, techniques in manufacturing, test and assembly of the off-axis freeform optical system are becoming more and more mature in recent years, which in turn lowers the difficulty and cost of the system.

5 Conclusion

A two-mirror off-axis SA optical system with an entrance pupil of 100 mm is proposed. The spherical primary mirror consists of three identical sub-mirrors which are arranged in the Golyay3 configuration. The surface of the secondary mirror has a freeform surface described by the X - Y polynomials to balance the spherical and off-axis aberrations. Both the primary and secondary mirrors are tilted to avoid the central obstruction. The fill factor of the final off-axis system is 58.4%, which is much larger than that of an on-axis system. The aperture stop which serves as a baffle is located at 760 mm from the primary mirrors to more easily control the amount of entry light. With the optimization using the optical design software ZEMAX, the off-axis Golyay3 SA system achieves a 2.5° full diagonal FOV.

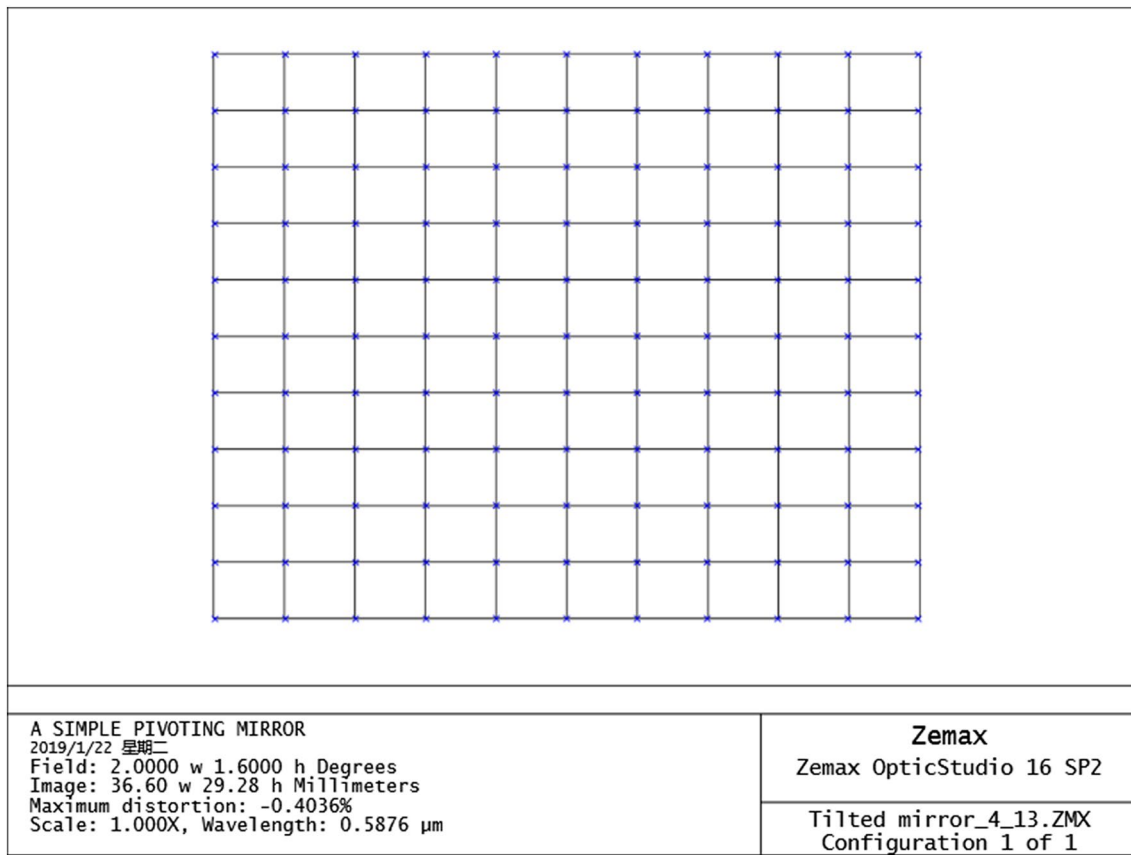


Fig. 9 Grid distortion of the off-axis Golay3 SA system

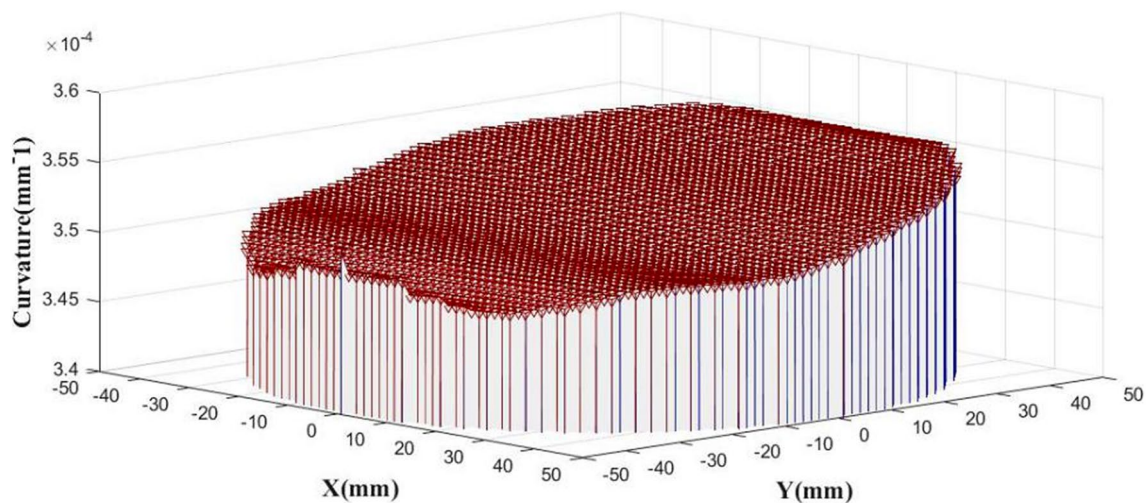


Fig. 10 Curvature variation of the secondary mirror

Acknowledgements This work is supported partially by National Science Foundation of China (NSFC) (61875145, 11804243); Jiangsu Province Key Discipline of China’s 13th 5-year plan (20168765); Jiangsu Key Laboratory of Advanced Optical Manufacture Technology (KJS1710); Suzhou Key Laboratory (SZS201611, SZS201712); and

the Six Talent Peaks Project of the Jiangsu Province (DZXX-026). The authors are also grateful to Professor Qian Lin of Soochow University for valuable advices and to Dr. Cao Zongjian of Augusta University in USA for editorial suggestions.

References

1. Robert, D.F., Theodore, A.T.: Image quality of sparse-aperture designs for remote sensing. *Opt. Eng.* **41**(8), 1957–1968 (2002)
2. Genet, R., Rowe, D., Clause, M.: Sparse-aperture quasi-meridian telescopes. *J. Double Star Obs.* **12**, 287–294 (2016)
3. Johns, M., Mccarthy, P., Raybould, K.: Giant magellan telescope: overview. *Proc. SPIE* **8444**(1), 84441H_1–84441H_16 (2012)
4. Xie, Z.L., Ma, H.T., Qi, B.: Experimental demonstration of enhanced resolution of a Golay3 sparse-aperture telescope. *Chin. Opt. Lett.* **15**(4), 041101_1–041101_4 (2017)
5. Harvey, J.E., Ftaclas, C.: Field-of-view limitations of phased telescope arrays. *Appl. Opt.* **34**(25), 5787–5798 (1995)
6. O. Lardière, Martinache, F., Patru, F.: Direct imaging with highly diluted apertures—I. Field-of-view limitations. *Mon. Not. R. Astron. Soc.* **375**(3), 977–988 (2018)
7. Ardenne, A.V., Bregman, J.D., Cappellen, W.A.V.: Extending the field of view with phased array techniques: results of European SKA research. *Proc. IEEE* **97**(8), 1531–1542 (2009)
8. Salvaggio, P.S., Schott, J.R., McKeown, D.M.: Validation of modeled sparse aperture post-processing artifacts. *Appl Opt.* **56**(4), 761–770 (2017)
9. Kuhn, J.R., Moretto, G., Racine, R., et al.: Concepts for a large-aperture, high dynamic range telescope. *Publ. Astron. Soc. Pac.* **113**(790), 1486–1510 (2001)
10. Moretto, G., Kuhn, J.R.: Highly sensitive telescope designs for higher contrast observations. *Adv. Opt. Technol.* **3**(3), 251–264 (2014)
11. Kuhn, J.R., Hawley, S.L.: Some astronomical performance advantages of off-axis telescopes. *Publ. Astron. Soc. Pac.* **111**(759), 601–620 (1999)
12. Wynne, C.G.: Field correctors for very large telescopes. *Mon. Not. R. Astron. Soc.* **280**(2), 555–558 (2018)
13. Gautam, S., Gupta, A., Singh, G.S.: Optical design of off-axis Cassegrain telescope using freeform surface at the secondary mirror. *Opt. Eng.* **54**(2), 025113 (2015)
14. Yabe, A.: Method to allocate freeform surfaces in axially asymmetric optical system. *Proc. SPIE* **8167**(4), 816703_1–816703_10 (2011)
15. Luttrell, D.E.: Machining non-axisymmetric optics, in *ASPE Proceedings* (ASPE, Rochester, 1990), pp. 31–34
16. Forbes, G.W.: Shape specification for axially symmetric optical surfaces. *Opt. Express* **15**(8), 5218–5226 (2007)
17. Pan, J.H.: *The design, manufacture and test of the aspherical optical surfaces*, Soochow University Press., pp. 32–35 **Su Zhou(2004)**

Publisher's Note Springer Nature remains neutral with regard to jurisdictional claims in published maps and institutional affiliations.